

Manipulating the Coffee-Ring Effect: Interactions at Work

Manos Anyfantakis ^{*,[a, b, c]} and Damien Baigl ^{*,[a, b, c]}

In memory of Zheng Geng

The evaporation of a drop of colloidal suspension pinned on a substrate usually results in a ring of particles accumulated at the periphery of the initial drop. Intense research has been devoted to understanding, suppressing and ultimately controlling this so-called coffee-ring effect (CRE). Although the crucial role of flow patterns in the CRE has been thoroughly investigated, the effect of interactions on this phenomenon has been largely neglected. This Concept paper reviews recent works in this field and shows that the interactions of colloids with (and at) liquid–solid and liquid–gas interfaces as well as bulk particle–

particle interactions drastically affect the morphology of the deposit. General rules are established to control the CRE by tuning these interactions, and guidelines for the rational physicochemical formulation of colloidal suspensions capable of depositing particles in desirable patterns are provided. This opens perspectives for the reliable control of the CRE in real-world formulations and creates new paradigms for flexible particle patterning at all kinds of interfaces as well for the exploitation of the CRE as a robust and inexpensive diagnostic tool.

1. Introduction

Particle deposition from evaporating drops of liquids containing non-volatile solutes phenomenologically seems to be a rather uncomplicated problem. However, our everyday experience contrasts intuition. Characteristic ring-shaped deposits are observed after the drying of spilled coffee or tea drops. Washed tableware displays white stains of the same morphology, since salt crystals accumulate at the edge of the water drops after drying. Rain drops also leave rings of dust particles after drying on windows. Surprisingly, the omnipresent effect responsible for the formation of the above-mentioned patterns, frequently referred to as the coffee-ring effect (CRE), was elucidated only less than two decades ago. Deegan et al.^[1] explained that, in volatile liquid droplets partially wetting a solid substrate, the evaporation rate has its maximum close to their pinned three-phase contact line. This inhomogeneous evaporation profile results in the development of a radial fluid flow from the interior of the drop to the contact line, to replenish the liquid lost there. Solutes present in the liquid are transported by the flow and are deposited at the edge of the drop; their progressive accumulation leads to the formation of ring-shaped patterns after drying is complete.

[a] Dr. M. Anyfantakis, Prof. D. Baigl
Ecole Normale Supérieure-PSL Research University
Department of Chemistry
24 rue Lhomond, 75005, Paris (France)
E-mail: emmanouil.anyfantakis@ens.fr
damien.baigl@ens.fr

[b] Dr. M. Anyfantakis, Prof. D. Baigl
Sorbonne Universités
UPMC Univ Paris 06, PASTEUR
75005, Paris (France)

[c] Dr. M. Anyfantakis, Prof. D. Baigl
CNRS, UMR 8640 PASTEUR
75005, Paris (France)

1.1. Motivation for Studying the CRE

Understanding and controlling solute deposition from evaporating liquids is a key factor in various technologies, such as inkjet printing,^[2] DNA and protein microarrays^[3,4] and micro-patterning,^[5] which explains the intense research effort in the last two decades for revealing the underlying phenomena in a seemingly curiosity-driven research topic.^[6]

From a purely scientific point of view, the CRE offers a rich physicochemical platform for the investigation of numerous, complex and usually entangled phenomena. Microscopic effects, such as particle–particle and particle–interface interactions, macroscopic effects, such as flow patterns, and phenomena simultaneously involving different length scales, such as wetting, are all integrated in a challenging physical problem.^[7] In addition, the robust and persistent character of the CRE makes it very intriguing. The primary requirements for the CRE to take place—volatile liquid, finite contact angle, and pinned contact line—are commonly met in the majority of practical systems and applications, and this accounts for its ubiquitous nature.^[1] Moreover, it occurs in a wide range of drop sizes (diameters ranging from micrometers to centimeters)^[8,9] and in a plethora of systems with diverse chemical properties and various characteristic length scales. Examples include molecular (i.e. salt)^[8] and macromolecular solutions,^[10] colloidal suspensions (particle sizes from nanometers to micrometers)^[11] and biomaterial-based complex fluids (e.g. blood, protein solutions, and biofilms^[11–13]).

1.2. Strategies for Controlling the CRE

A significant part of research studies devoted to the CRE was focused on uncovering the physicochemical parameters affecting evaporative particle deposition and particularly on devising

strategies for suppressing the effect and achieving homogeneous solute deposition. Given that evaporation-driven flow toward the pinned contact line is always present in a volatile sessile drop, the vast majority of these approaches was based on affecting the hydrodynamics of drying drops. Different additives, including surfactants,^[10,14] polymers,^[15] cosolvents^[2] and nanoparticles,^[16] were introduced to manipulate the flow patterns in evaporating drops. External methods that require no additives, such as electrowetting^[17] and exposure of the drying drops to vapours of miscible, low-surface-tension liquids,^[18] have also been successfully utilised. Other approaches relied on the addition or removal of deposited matter by mechanical means.^[19]

1.3. Scope and Organisation of this Paper

The interconnection between flow patterns and final deposit morphology has been recently described in detail in an instructive review by Larson.^[7] The scope of this Concept paper is primarily to underline the generally overlooked but highly important influence of interactions on deposition patterns emerging from evaporating drops. In particular, we focus on the interactions of the suspended particles with/at the liquid-gas (LG) and liquid-solid (LS) interfaces, as well as bulk particle-particle interactions. In drying drops of most complex liquids, the morphology of the final deposits is determined by both the hydrodynamics (i.e. flow patterns) and the interactions present in the system (Figure 1). This is expectable con-

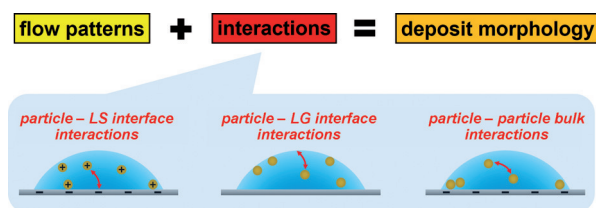


Figure 1. The two key elements dictating deposit morphology from evaporating sessile drops of colloidal suspensions: flow patterns and interactions. The latter, which are at the focus of this paper, include interactions of the suspended particles with the LS and LG interfaces, as well as bulk particle-particle interactions.

sidering that most of interactions involving colloids and interfaces (e.g. Coulomb and van der Waals interactions, capillary forces, hydrophobic interactions) can typically exceed the thermal energy and therefore can strongly affect particle organisation and behaviour at interfaces.

The paper is structured as follows. Selected recent publications that have explored the effect of interactions of different nature are highlighted in Section 2. After analysing the role of the interactions with/at the LS (Section 2.1) and LG (Section 2.2) interfaces, we analyse the effects of bulk particle-particle interactions (Section 2.3) prior to providing a list of general guidelines to control particle patterning from drying drops (Section 2.4). Next, we describe a few paradigms in which these interactions have been exploited for applications of practical importance (Section 3). In suspensions in which the parti-

cle affinity for the LG interface is optically tuned, particle deposition can be dynamically controlled by using light (Section 3.1). Moreover, we describe recently developed biosensing strategies based on dry patterns resulting from particle aggregation induced by the attraction between probe particles and the biomarker molecule to be detected, which open the way to low-cost and simple-to-operate point-of-care diagnostics (Section 3.2). Conclusions and perspectives are given in Section 4.

2. Interactions of Particles with/at Interfaces Affecting the CRE

A number of groups have investigated the effect of the various types of interactions in a drying drop of colloidal suspension on the resulting particle deposition. In the following, we categorise some of the most relevant publications based on the type of interaction: particle-LS interface, particle-LG interface and bulk particle-particle interactions. However, this classification is not mutually exclusive, since it is common that in a single publication, more than one of the above-mentioned types of interaction are investigated.

2.1. Interactions with the LS Interface (Substrate)

Bhardwaj et al.^[20] studied the role of the Derjaguin-Landau-Verwey-Overbeek (DLVO) interactions on the pattern morphology from evaporating nanoliter droplets of a suspension of titania nanoparticles deposited on glass. Variation of the suspension pH led to modification of the DLVO particle-substrate and particle-particle interactions, which in turn altered the shapes of the deposits. Evaporating drops at low pH values yielded a relatively homogeneous pattern consisting of a thin uniform nanoparticle layer with a thicker ring at the edge. Calculations showed that the particle-substrate DLVO force at low pH values was attractive. Particles in close proximity to the substrate were thus attracted to it and formed a uniform deposit (Figure 2a). Deposits obtained from drying drops at intermediate pH consisted of aggregates covering the whole initially wetted area. Near the point of particle neutral charge, the particle-substrate DLVO force was weaker than the interparticle van der Waals attraction, and hence particle aggregation occurred. At the highest pH values, drop drying led to a marked ring pattern with almost no particles in the area enclosed by the ring. In this pH region, strong repulsive particle-substrate forces prevented the nanoparticles from contacting the substrate, and they were carried along by the outward capillary flow to the drop contact line (Figure 2b).

A phase diagram was proposed for prediction of the deposit shape from evaporating drops. It was suggested that the deposit shape results from the competition of three transport mechanisms in the drop: 1) the outward capillary flow favouring ring-shaped deposits; 2) particle transport toward the substrate, driven by attractive DLVO interactions and promoting uniform deposits; and 3) a Marangoni recirculatory flow, driven by surface-tension gradients and favouring a central bump de-

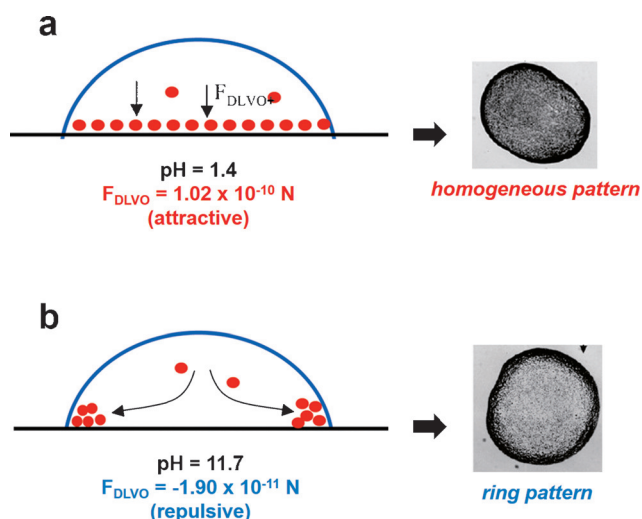


Figure 2. The influence of pH-dependent particle–LS interface (substrate) DLVO interactions on the deposit morphology from drops of titania nanoparticles drying on glass substrates. a) At low pH, particle–substrate interactions are attractive, promote particle adhesion at the substrate and eventually lead to a homogeneous deposit. b) At high pH, particle–substrate interactions are repulsive, and the evaporation-induced capillary flow brings particles to the contact line, where they form a ring-shaped pattern. Adapted with permission from Ref. [20]. Copyright 2010 American Chemical Society.

posit with a diameter much smaller than the initial drop diameter.

Yan et al.^[21] investigated the impact of particle and substrate charge on the colloidal self-assembly close to the edge of an evaporating sessile drop, in the absence and presence of surfactants, at concentrations below the critical micellar concentration (CMC). It was demonstrated that particle mobility, governed by the particle–substrate interactions, was a key parameter affecting particle ordering and deposition. For surfactant-free suspensions of particles having the same charge as the substrate, ring-shaped deposits consisting of significantly ordered self-assembled particles were observed. Contrarily, drops of particles on an oppositely charged substrate led to the formation of rings with an increased number of deposited particles in the drop interior. Attraction between the colloids and the LS interface resulted in decreased particle mobility and therefore disordered structures. In the presence of a nonionic surfactant, the self-assembly behaviour was similar to that of the surfactant-free systems. When a charged surfactant with the same charge as the particle and the substrate was added to the formulation, particle ordering and patterning were similar to those of the like-charged, surfactant-free systems. For oppositely charged particle–substrate systems, addition of a surfactant having the opposite charge to the particle promoted the formation of rings consisting of ordered self-assemblies. This was explained by surfactant adsorption to the particles, which decreased the particle charge density and therefore weakened adhesion to the LS interface. Finally, in the case of like-charged particle–substrate systems, addition of an oppositely charged surfactant led to strong adhesion of particles to the LS interface and thus promoted disorder. This effect was attributed to the hydrophobic attraction between the surfac-

tant layer adsorbed on the substrate and that adsorbed on the colloid surface.

Recently, Dugyala and Basavaraj investigated the influence of particle shape and DLVO interactions on the patterns formed by drying sessile droplets.^[22] They employed aqueous suspensions of hematite ellipsoids, a model system with adjustable particle aspect ratio (through synthesis) and surface charge (through pH variation). For a fixed aspect ratio of 4 and at low pH, hematite drops deposited on cleaned glass yielded rings enclosing an area covered with a mono- or multilayer of particles. Ring formation was attributed to the repulsive particle–particle interactions allowing particles to migrate to the drop edge, driven by the outward capillary flow. The deposition of some particles inside the area enclosed by the ring was ascribed to particle–substrate attraction. At intermediate pH, reduced Coulomb particle–particle repulsion and van der Waals interactions resulted in particle aggregation. At the same time, particle–substrate attraction led to the deposition of single particles and aggregates on the glass, and a uniform dry pattern was produced. At high pH, both particle–particle and particle–substrate interactions were repulsive and led to the formation of a ring pattern (Figure 3).

Independent of the particle aspect ratio and for drops drying on cleaned glass, rings were always observed for acidic and basic conditions, whereas homogeneous patterns were obtained for intermediate pH values. Surface-tension measure-

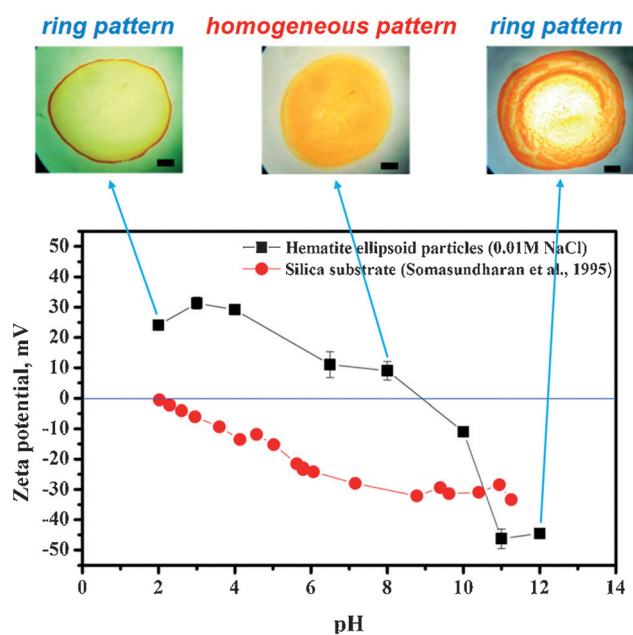


Figure 3. Deposition patterns from evaporating drops of hematite ellipsoids (fixed aspect ratio of 4) dispensed on glass substrates. At low pH, ring deposits enclosing mono- or multilayers of particles are formed due to the combination of particle–substrate attraction, particle–substrate repulsion and the outward capillary flow. At intermediate pH, reduced electrostatic interparticle repulsion and attractive van der Waals interactions cause aggregation. Attractive particle–substrate interactions lead to the deposition of single particles and aggregates on the substrate in a uniform pattern. Particle–particle and particle–substrate repulsion in conjunction with the outward flow resulted in ring deposits at high pH values. Adapted with permission from Ref. [22]. Copyright 2014 American Chemical Society.

ments in pendant drops of suspension in decane indicated that hematite particles were adsorbed at the water–decane interface for intermediate pH, whereas no adsorption occurred under acidic conditions. Surprisingly, at intermediate pH, the hydrophobicity of the substrate was found to determine the dry-deposit morphology. Whereas drops on cleaned (i.e. hydrophilic) glass yielded homogeneous patterns, drops on silanised glass led to the formation of rings. The authors concluded that, at intermediate pH, particle–substrate interaction was the dominant factor determining the pattern morphology: negligible interaction (hydrophobic substrates) led to coffee rings, whereas attraction (hydrophilic substrates) led to ring suppression, with particle adsorption to the free interface occurring in any case.

Morales et al.^[23] studied the influence of nonionic surfactants on the dry-pattern morphologies and the attachment strength of particles on the substrate from evaporating sessile drops. At high initial surface tensions (i.e. low initial surfactant concentrations), amorphous stains were observed, at intermediate initial surface tensions, coffee-ring patterns were obtained, and low surface tensions (i.e. high surfactant amount) resulted in patterns consisting of concentric rings. These morphologies were linked to three distinct drying regimes attributed to transitions of contact-line dynamics between slipping, pinned and recurrent slip–rip–stick states, respectively. The presence of the surfactant did not modify the van der Waals and Coulomb particle–substrate interactions. However, with increasing surfactant concentration, adsorption of micelles on the particle and substrate surfaces led to micelle-protrusion repulsion, which affected the interactions between the contact line and the particles and in turn influenced the deposition and attachment strength of particles on the substrate.

We have recently investigated the influence of the interactions between the suspended particles and the LS interface on the deposit morphology resulting from the drying of drops of aqueous colloidal suspension on glass substrates.^[24] Surfactant-free dispersions always led to the formation of ring deposits, since the majority of particles accumulated at the drop edge. However, the amount of particles deposited in the area encircled by the ring varied depending on the particle and substrate charge. For particles and substrates having the same charge, only a limited number of particles were deposited in the interior area. Contrarily, for oppositely charged particle–substrate pairs, electrostatic attraction led to the formation of rings enclosing an area covered with an increased number of colloidal particles. The addition of ionic surfactants (at concentrations lower than the CMC) was found to modify the electrostatic properties of the particles and the LS interface and therefore to modulate the amount of particles adsorbed on the glass.

2.2. Interactions with/at the LG Interface (Free Interface)

A motion opposing the CRE, driving solute accumulation at the center of evaporating drops, was described by Weon and Je,^[25] who experimentally observed that the initial evaporation-driven particle transport toward the contact line was reversed,

driving particles from the edge to the centre of the drop. This inward motion was attributed to capillary forces exerted on the suspended particles when the latter were in contact with the LG interface during drying, caused by the geometrical constraints, that is, the LG interface, the contact line and the contact angle, given that no particle protrusion from the free interface was observed.

Arrays displaying long-range order (over several micrometres) were obtained from drying drops of dodecanethiol-coated gold nanocrystals dispersed in toluene.^[26] Although initially thought to be the result of particle–particle and particle–substrate interactions as well as wetting of the liquid on the solid surface,^[26] later studies involving in situ small-angle X-ray scattering demonstrated that highly ordered 2D superlattices were formed at the LG interface of the evaporating drop.^[27] The formation of the 2D superlattices was explained by a kinetic “crushing” model describing the accumulation of nanocrystals at the descending LG interface. Bigioni et al.^[28] further showed that a sufficiently high flux to the LG interface (controlled by evaporation rate and particle concentration) and a sufficiently strong particle–interface interaction were required to create 2D islands, the formation of which was a prerequisite for macroscopic monolayer formation at later drying stages.

The shape of suspended particles was shown by Yunker et al. to be a crucial factor determining the morphology of evaporative deposits.^[29] The authors utilised dispersions of polystyrene spheres stretched asymmetrically to different aspect ratios α . During drop drying, spherical or slightly deformed particles ($\alpha = 1.0\text{--}1.1$) were efficiently transported to the pinned contact line by the outward capillary flow, and a typical ring was formed (Figure 4a and b). On the contrary, evaporation of drops of suspension consisting of more anisotropic particles ($\alpha > 1.1$) led to the formation of a pattern displaying uniform coverage (Figure 4c). The ellipsoidal particles were only transported toward the drop periphery until they reached the LG interface. After being carried there, the ellipsoids experienced long-range attraction between each other, because they deformed the LG interface. These strong attractions resulted in the formation of loosely packed, arrested structures at the interface, which gave rise to a high surface viscosity and enabled the colloids to resist the outward flow (Figure 4d). The strength and range of the particle–particle capillary interactions were decreased by the addition of surfactant to the drops. This enabled ellipsoids to pack closely at the contact line, since they were more flexible toward rearrangement at the interface, and eventually resulted in the formation of a ring pattern after drying. Drop evaporation of mixtures of spheres with ellipsoids resulted in uniform patterns, provided that the sphere diameter was larger than the minor axis of the ellipsoid. This effect was ascribed to the hindered motion of large spheres under or through the loosely packed particle structures, which prevented the former from reaching the contact line.

We have recently reported on the effect of surfactants on the deposition patterns from evaporating drops of colloidal dispersion on glass substrates at concentrations lower than the CMC.^[24] We demonstrated that the surfactant-mediated in-

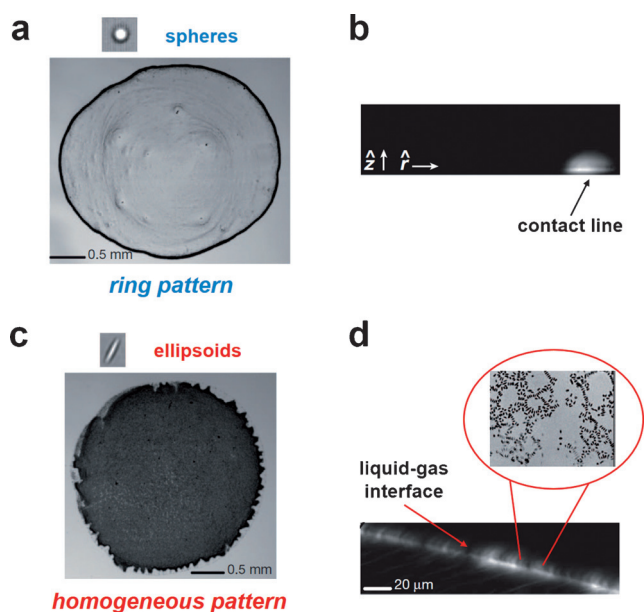


Figure 4. Colloidal shape influences interactions of particles with/at the LG interface and therefore deposit morphology in drying drops. a) Drops of suspensions of spherical colloids result in a typical ring pattern, since most of the particles are gathered at the drop edge due to the evaporative capillary flow (b). c) In stark contrast to spheres, drops containing ellipsoidal particles yield homogeneous patterns. Particles reaching the LG interface experience long-range attractions and form loosely packed networks, which enable particles to resist the evaporation-driven flow (d). Adapted with permission from Macmillan Publishers Ltd: Nature (Ref. [29]), copyright 2011.

teractions between the suspended particles and the LG interface are the key factor determining the morphology of the dry pattern (Figure 5). For like-charged particle/surfactant mixtures, the majority of the particles accumulated at the drop edge, forming ring patterns. A markedly different behaviour was shown for oppositely charged mixtures, whereby electrostatically driven surfactant adsorption to the particle surface was responsible for the enhanced particle affinity to the LG interface. For low surfactant concentrations, surfactant adsorption to the particle surface was limited, and ring patterns were always observed upon drying (Figure 5 a).

For intermediate concentrations, surfactant-coated particles became almost neutral and at the same time more hydrophobic, due to exposure of the apolar tails of the surfactant to the water phase. This in turn led to particle adsorption at the LG

interface, presumably due to hydrophobic interactions. Particle trapping and aggregation at the free interface led to the formation of a skin phase, the deposition of which resulted in homogeneous, disc-shaped dry patterns (Figure 5 b). With a further increase in surfactant concentration, particles were overcharged by the surfactant and again became hydrophilic; coffee ring deposits were once again formed after drop evaporation. Notably, we showed that the evolution of the deposit pattern followed a reproducible and general trend for a variety of particle/surfactant systems. Below the CMC, like-charged systems always led to rings, whereas oppositely charged systems displayed a ring–disc–ring evolution with the disc morphology systematically occurring at intermediate surfactant concentrations that closely corresponded to neutralisation of the particle surface charge (zeta potential around zero). Exploiting a similar concept, we recently demonstrated the dynamic control of particle deposition from evaporating drops using light,^[30] which is described in more detail in Section 3.1.

2.3. Bulk Particle–Particle Interactions Affecting the CRE

In Section 2.1, devoted to the role of the particle–LS interactions, we already described some examples in which the influence of bulk interparticle attraction/repulsion on the deposit shape had to be taken into account.^[20,22] In this section, we focus on other studies in which the role of particle–particle interactions was considered to be the predominant factor driving the deposition behaviour.

Talbot et al. quantitatively investigated the effect of viscoelastic properties of aqueous suspensions of polystyrene particles and laponite, a disc-shaped nanoparticle, on the deposit

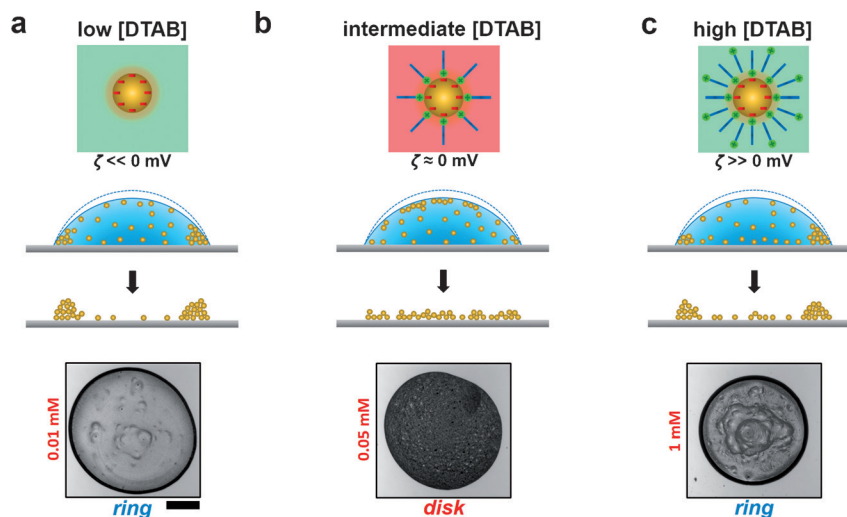


Figure 5. The effect of surfactant-mediated particle–LG interface interactions on the pattern morphology from evaporating drops of anionic particle–cationic surfactant mixtures. a) At zero or low surfactant concentration, particles remain anionic and hydrophilic due to zero or limited surfactant adsorption on their surface. The evaporation-driven convective flow leads to the formation of rings. b) At intermediate surfactant concentrations, surfactant adsorption leads to neutralisation and hydrophobisation of the particles. Trapping and aggregation of the particles at the LG interface creates a particle skin, the deposition of which leads to a homogeneous disc-shaped deposit. c) At high surfactant concentrations, surfactant molecules form a bilayer at the surface of the particles, which become cationic and hydrophilic. The outward convective flow leads to the formation of rings once again. Adapted with permission from Ref. [24]. Copyright 2015 American Chemical Society.

morphologies after the drying of inkjet-deposited droplets.^[16] Laponite was introduced to induce a sol–gel transition in the drying drops, which transforms the liquid from an initially stable colloidal dispersion to a soft gel. Gelation occurred owing to the growth of a laponite network spanning the liquid volume, which arose from the connections between the laponite particles as their concentration increased during evaporation. In particular, the authors suggested exploiting the elasticity rather than the viscosity enhancement caused by the sol–gel transition. By varying the initial concentration of laponite in a suspension with a fixed concentration of polystyrene particles, the gelling time and therefore the amount of convective radial flow could be adjusted, and thus the final deposition pattern could be controlled.

Without the addition of laponite, the convective radial flow dominated and ring-shaped deposits were formed (Figure 6a,

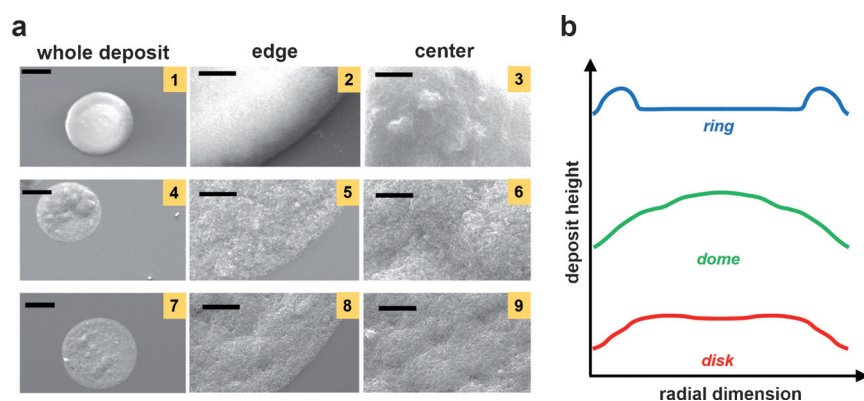


Figure 6. The effect of laponite-induced gelation on the deposit formation from evaporating drops containing a fixed amount of polystyrene nanoparticles. a) SEM images and b) corresponding schematic deposit height profiles. 1–3: Laponite-free drops lead to the formation of ring-shaped deposits, because most of the particles accumulate at the drop periphery due to the convective flow. 4–6: Addition of 2 wt% laponite leads to fast gelation, which rapidly suppresses the convective flow and produces a dome-shaped deposit. 7–9: A moderate amount of convective flow is achieved by slower gelation, which is realised by utilising a lower laponite concentration (1 wt%). Drying drops in this case led to the formation of homogeneous disc-shaped dry patterns. Adapted with permission from Ref. [16]. Copyright 2014 American Chemical Society.

1–3). In suspensions containing small amounts of laponite, a sol–gel transition occurred after a certain amount of time (controllable by means of the laponite concentration), with the drops first gelling at their edge and the gelation front propagating toward the centre. The moderate amount of radial flow led to the formation of homogeneous, pancake-like deposit morphologies (Figure 6a, 7–9). When higher laponite concentrations were utilised, the radial flow was suppressed very soon after drop deposition due to fast gelation; finally, dome-like deposits were obtained (Figure 6a, 4–6). Although the addition of laponite successfully homogenised the deposition patterns, it also led to aggregation of the polystyrene colloids. This aggregation was inhibited by adding silica nanoparticles to the suspensions. This study clearly illustrated how particle–particle interactions in the bulk could directly influence the local structure and the overall morphology of the deposits resulting from drying picoliter droplets.

Crivoi and Duan studied the effect of hexadecyltrimethylammonium bromide on the deposit morphology obtained by evaporating droplets of dispersed aluminium oxide nanoparticles on Si wafers.^[31] In the surfactant-free dispersions, particles tended to aggregate into clusters, which upon drying deposited into a uniform layer enclosed by a visible ring. Addition of surfactant reduced particle aggregation and led to the formation of typical ring patterns, with only a limited number of nanoparticles deposited in the pattern interior. The particle–substrate attraction was comparable for the surfactant-free and surfactant-containing dispersions and did not play a major role in the pattern morphology. The authors developed a model based on diffusion-limited cluster–cluster aggregation to qualitatively explain the experimental results. By varying the particle sticking probability from 0 to 100%, a continuous transformation from a coffee ring to a uniform pattern was observed in the simulations. Therefore, controlling the particle sticking probability by modifying the fluid properties (in this case by the addition of surfactants) offered a way to manipulate the self-assembly patterns formed from evaporating drops.^[31]

The concept of using the LG interface of a drying droplet as a tool for directing the assembly of colloids into microscopic objects displaying long-range order was demonstrated by Kuncicky and Velev.^[32] The shape of the templating free interface and thus the morphology of the final assemblies were determined by the dynamics of the receding contact line. The drop contact angle, the initial particle concentration and the amount of electrolyte were employed as the

parameters controlling the contact-line dynamics. The morphologies of dry microstructures fell into two categories. Convex structures displaying a spherical cap (convex) shape and ring-shaped (concave) structures dimpled inward were observed, depending on the substrate wettability and the initial volume fraction of the particles. To correlate the electrostatic particle–particle and particle–substrate interactions to the drying dynamics and the resultant deposit morphology, the researchers examined the effect of added electrolyte in drops drying on hydrophobic substrates. For low salt concentrations, particles adhered to the substrate during drying, and this led to the pinning of the contact line, which was initially free to recede. The final pattern had the form of a spherical cap. At intermediate concentrations, the contact line was pinned during the whole lifetime of the drop. The particles in the vicinity of the free interface coagulated and created a shell; the dry deposit consisted of the crumpled shell. Finally, high ionic strength led to enhanced particle aggregation and sedimenta-

tion, which resulted in a “sand-pile” micropatch. Besides the salt-induced screening of the electrostatic repulsions, the authors noted that hydrophobic attractions could also contribute to the adhesion of particles to the substrate.

2.4. General Guidelines for Controlling Patterns from Evaporating Drops

Particle patterning from drying drops is generally a complex process, accompanied by additional complications specific to each liquid used. However, from the studies described above, we conclude that some general guidelines for controlling evaporative patterning do exist and it would be useful to list them here. These guidelines are based on the interactions between the components of a drying drop, that is, the particles and the interfaces. Regarding particle–LG interface interactions, it has been shown that both neutralisation and hydrophobisation of the particles promotes their affinity for that interface. This commonly leads to particle trapping at the LG interface and the formation of interfacial aggregates, which have a profound effect on the morphology of the dry pattern. The general trend is that promoting particle trapping at LG interface hinders ring formation and favours disc-like deposits with a variable degree of homogeneity. So far, this has been achieved: 1) by the addition of oppositely charged surfactants in a precise concentration range leading to the adsorption of a surfactant monolayer that causes particle neutralisation and 2) by adjusting the pH of the liquid, which determines the degree of protonation/deprotonation of the surface groups. We anticipate that other candidates, such as molecular electrolytes (through the screening of the electrostatic interactions) or polyelectrolytes (through electrostatically driven particle coating) could lead to similar phenomena and we think they are worthy of systematic studies. Another scientific challenge is to discriminate the exact contribution of each of the two main components, electrostatic and hydrophobic interactions, which are entangled in many experimental systems.

Considering particle–LS interface interactions as the platform for guiding evaporative particle deposition, we have shown that, regardless of their origin (Coulomb, van der Waals or hydrophobic), attractive interactions with the LS interface promote pattern homogenisation from drying drops. There is thus a strong analogy between the role of LG and LS interfaces in directing the deposition behavior: particle affinity for any of these interfaces competes with the outward capillary flow and promotes uniform deposition. However, the nature, range and intensity of the interactions at work can be very different between these two interfaces. For instance, long-range capillary forces, which are specific to the LG interface, were shown to be instrumental in directing the deposition behaviour. Conversely, long-range electrostatic interactions can be easily tuned in the specific case of the LS interface, by simple surface modifications.

Finally, modulating particle–particle interactions can significantly affect evaporative particle deposition as well. Generally, in drops of suspensions of poorly stabilised colloids, aggregation leads to clustering. When the cluster size is large enough,

sedimentation can lead to an overall uniform but locally inhomogeneous deposit morphology. Alternatively, the viscoelastic properties of nanoparticle dispersions that are prone to gelation can be exploited for the even patterning of co-suspended particles, which provides a successful route to homogenised deposits.

The existence of the above-mentioned general rules relating the interactions in an evaporating drop and the resulting deposit morphology open the way to the exploitation of this relation for practical applications. A few examples toward this end are described in Section 3.

3. Exploiting Interaction-Driven Particle Deposition

The direct relation between the interactions occurring in an evaporating drop and the morphology of the dry deposit from evaporating drops can be exploited in two ways. On the one hand, on-demand tuning of the relevant interactions in a drying drop can lead to tailored particle patterning. Conversely, characterisation of the deposited pattern can give valuable information about the interactions taking place in a drying drop of a multicomponent liquid (Figure 7a). Paradigms exploiting this bidirectional nature of the interactions–deposit relation are presented below.

3.1. Tailored Particle Deposition at Interfaces

We recently reported on the design of photoresponsive colloidal suspensions by mixing anionic polystyrene particles with the photosensitive cationic surfactant AzoTAB, which consists of a polar head group and a hydrophobic tail with an azobenzene moiety. By irradiating with blue ($\lambda = 440$ nm) or UV ($\lambda = 365$ nm) light, the isomeric state of AzoTAB could be reversibly changed between *trans* (less polar, less hydrophilic) and *cis* (more polar, more hydrophilic), respectively. This had a direct consequence for the amount of surfactant molecules bound on the particle surface: for a fixed particle concentration, a larger amount of *trans*-AzoTAB surfactant molecules were adsorbed on the particle surface compared to the *cis* isomer. This enabled us to finely and reversibly tune the particle surface properties (charge and hydrophobicity) and therefore their interaction with the LG interface, solely by irradiation with light, while keeping the liquid composition unchanged.^[30]

In a way analogous to the case of common (i.e. non-photo-sensitive) surfactants, particle trapping and clustering at the LG interface could be triggered by light by exploiting particle neutralisation and hydrophobisation induced by light-dependent adsorption of AzoTAB on the particles. Drying of an irradiated single drop could reversibly yield a ring or a homogeneous disc pattern, depending on the wavelength used. Spatial control of evaporative deposition in an array of multiple identical drops could be achieved by utilising structured light patterns by means of a simple photomask (Figure 7b). Notably, by adjusting the irradiation time, we were able to finely control the amount of particles deposited at the drop edge and its interior, and therefore to precisely adjust the degree of homogeneity

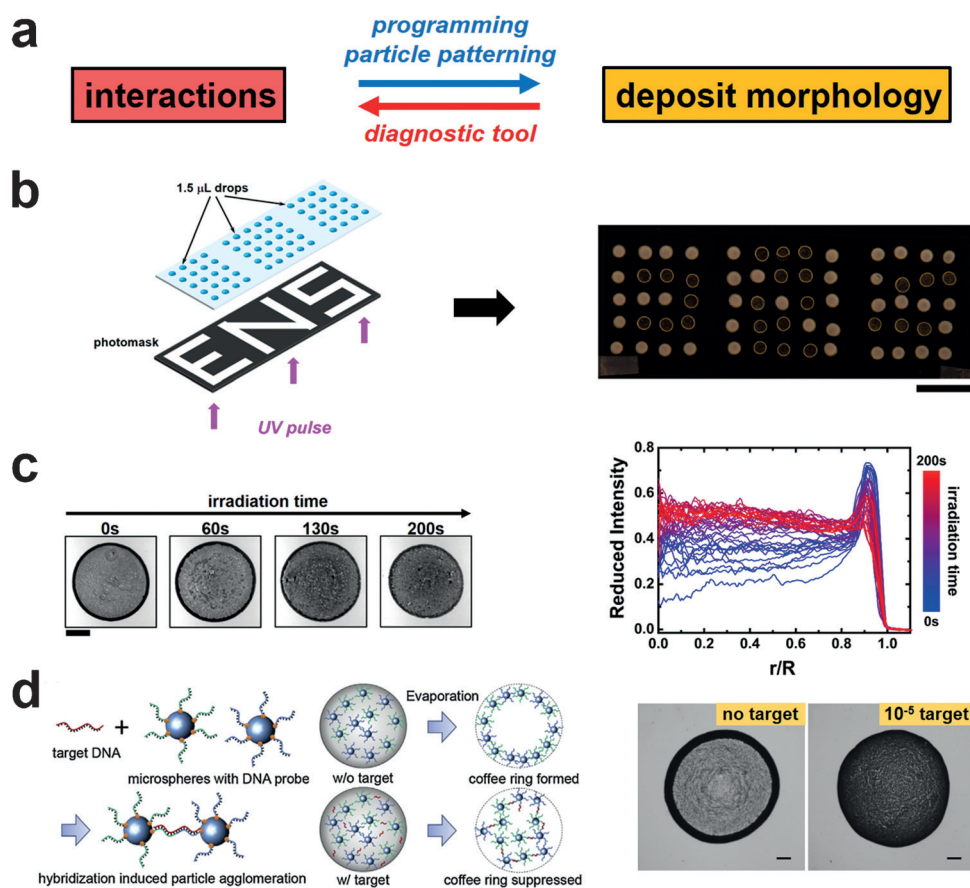


Figure 7. a) The interactions/deposit morphology relation can be harnessed for programming desired particle deposition on substrates or as a straightforward and low-cost diagnostic tool. b) Photocontrol of the CRE in drying drops containing nanoparticles and photosensitive surfactants. Spatial control of colloidal deposition in an array of multiple drops by means of a simple photomask. Adapted with permission from Ref. [30]. c) Temporal control of deposited particle distribution from an evaporating drop. The distribution of deposited particles can be tuned on demand simply by adjusting the irradiation time. Reprinted with permission from Ref. [30]. d) Detection of a target DNA molecule based on the hybridisation-induced suppression of the CRE. Simultaneous hybridisation of the target DNA with two colloidal particles functionalised with probe oligonucleotides complementary to the target DNA leads to the formation of a homogenous deposit. On the contrary, the absence of the target DNA results in the formation of a typical coffee-ring pattern. Reprinted from Ref. [33], with permission from Elsevier.

in the final deposit (Figure 7c).^[30] This is the first example in which the morphology of the pattern resulting from an evaporating drop could be dynamically tuned at constant drop composition, since we demonstrated photoreversible switching between marked rings and homogenous patterns.

We thus believe that such particles with optically tunable affinity for the LG interface provide a starting point for the programmable patterning of colloids. An interesting perspective is the possibility of intradrop patterning, that is, the controlled formation of topological features inside a single drop by using optical patterns. Research in this direction is currently ongoing in our group and preliminary results are encouraging.

3.2. Patterns from Evaporating Drops as a Diagnostic Tool

The possibility of exploiting the deposition patterns resulting from drying drops as a tool to detect target molecules in biological fluids has recently attracted scientific interest. Li et al.^[33] presented an easy and highly efficient method to detect

a target nucleic acid molecule that relied on the hybridisation-induced suppression of the CRE. They employed suspensions of polystyrene microparticles functionalised with two different probe oligonucleotides that were complementary to the target DNA. When the latter was present in solution, simultaneous hybridisation of the target DNA with the two probes occurred and led to agglomeration through microparticle bridging. Anisotropic aggregates trapped at the LG interface caused distortion of the surrounding meniscus, which resulted in long-range attraction to other aggregates. This in turn led to the gradual formation of a network at the free interface, which prevented particles from forming a ring structure at the drop contact line, and the CRE was eventually suppressed. On the contrary, when the target DNA was present at concentrations below the detection limit of this method ($\approx 10^{-8} \text{ mol L}^{-1}$), a typical ring pattern was observed, since (non-aggregated) particles were free to be transported to the drop edge by the radial convective flow (Figure 7d). By simple image processing, these authors were able to measure the extent of coffee-ring suppression and

therefore to quantify the concentration of the present target DNA. Besides its effective sensitivity, this method is highly specific in that it can distinguish sequences with a single mismatched nucleotide.

Another interesting example that made use of the morphology of the deposited pattern to extract information about the presence of a target molecule in a liquid sample was recently reported by Trantum et al.^[34] The detection strategy was based on the combination of Marangoni flows and target-mediated particle aggregation. The utilised particles were functionalised with a M13 monoclonal antibody able to bind to the M13K07 bacteriophage, which was the target molecule. Colloids remained dispersed or were aggregated when the bacteriophage was absent or present in solution, respectively. In the former case, particles were transported to the contact line by Marangoni flow from the drop apex to the drop edge. Contrarily, in the presence of the bacteriophage, large aggregates settled to the substrate, resulting in particle accumulation in the centre of the drop. The biosensor signal, based on the spatial distribu-

tion of the deposited particles upon drop evaporation, could be easily measured by means of optical microscopy. A deposit with only a small amount of particles gathered at the centre of the drop corresponded to a negative test (indicating the absence of the target molecule), whereas a deposit with a large spot at the centre corresponded to a positive test.

4. Conclusions and Perspectives

The take-home message of this Concept paper is that, in combination with flows, the interactions between the components of particle-laden drops (particles and interfaces) define the characteristics of the deposition pattern after drying. This interaction–deposit morphology relation can be exploited in two directions: 1) the programmable patterning of particles from drying drops and 2) as a diagnostic tool to gather information about the physics/chemistry taking place between the components of a drop.

Regarding the former, the vivid scientific interest of the last two decades has led to valuable accumulated knowledge of the interconnected effects occurring in a drying drop that directly impact the deposition pattern. However, increasing the complexity of the drop liquids, required for the development of new applications, calls for an improvement of our understanding. Such an achievement may provide a complete toolbox for the programmable and possibly complex patterning of solutes at all kinds of interfaces (fluid–solid, fluid–fluid, curved, flat). We believe that the strong interplay between the interactions (particle–particle and particle–interface) taking place inside a drying drop and the final morphology of the dry pattern makes possible the development of “coffee-ring diagnostics”, a field in which looking at deposit morphological features will provide qualitative to quantitative information about the interactions occurring in the drop to be analysed. For physico-chemical investigations, this will allow researchers to estimate the strength of interactions in situations in which classical methods become inappropriate. For societal and healthcare applications, we think that analysing the CRE of samples of biomedical interest will become a main player in the booming development of point-of-care diagnostic testing.

Acknowledgements

This work was supported by the European Research Council (ERC) [European Community's Seventh Framework Programme (FP7/2007-2013)/ERC Grant agreement n° 258782] and the Mairie de Paris [Emergence(s) 2012]. M.A. acknowledges funding from the European Commission (FP7-PEOPLE-2013-IEF/Project 624806 “DI-OPTRA”).

Keywords: aggregation • coffee-ring effect • colloids • evaporation • interfaces

- [1] R. D. Deegan, O. Bakajin, T. F. Dupont, G. Huber, S. R. Nagel, T. A. Witten, *Nature* **1997**, *389*, 827–829.
- [2] J. Park, J. Moon, *Langmuir* **2006**, *22*, 3506–3513.
- [3] Y. Deng, X.-Y. Zhu, T. Kienlen, A. Guo, *J. Am. Chem. Soc.* **2006**, *128*, 2768–2769.
- [4] R. Blossley, A. Bosio, *Langmuir* **2002**, *18*, 2952–2954.
- [5] H. Ma, J. Hao, *Chem. Soc. Rev.* **2011**, *40*, 5457–5471.
- [6] R. G. Larson, *Angew. Chem. Int. Ed.* **2012**, *51*, 2546–2548; *Angew. Chem.* **2012**, *124*, 2596–2598.
- [7] R. G. Larson, *AIChE J.* **2014**, *60*, 1538–1571.
- [8] R. D. Deegan, O. Bakajin, T. F. Dupont, G. Huber, S. R. Nagel, T. A. Witten, *Phys. Rev. E* **2000**, *62*, 756–765.
- [9] X. Shen, C.-M. Ho, T.-S. Wong, *J. Phys. Chem. B* **2010**, *114*, 5269–5274.
- [10] T. Kajiyama, W. Kobayashi, T. Okuzono, M. Doi, *J. Phys. Chem. B* **2009**, *113*, 15460–15466.
- [11] T. S. Wong, T. H. Chen, X. Shen, C. M. Ho, *Anal. Chem.* **2011**, *83*, 1871–1873.
- [12] W. Sempels, R. De Dier, H. Mizuno, J. Hofkens, J. Vermant, *Nat. Commun.* **2013**, *4*, 1757.
- [13] D. Brutin, B. Sobac, B. Loquet, J. Sampol, *J. Fluid Mech.* **2010**, *667*, 85–95.
- [14] T. Still, P. J. Yunker, A. G. Yodh, *Langmuir* **2012**, *28*, 4984–4988.
- [15] L. Cui, J. Zhang, X. Zhang, L. Huang, Z. Wang, Y. Li, H. Gao, S. Zhu, T. Wang, B. Yang, *ACS Appl. Mater. Interfaces* **2012**, *4*, 2775–2780.
- [16] E. L. Talbot, L. Yang, A. Berson, C. D. Bain, *ACS Appl. Mater. Interfaces* **2014**, *6*, 9572–9583.
- [17] H. B. Eral, D. M. Augustine, M. H. G. Duits, F. Mugele, *Soft Matter* **2011**, *7*, 4954–4958.
- [18] M. Majumder, C. S. Rendall, J. A. Eukel, J. Y. L. Wang, N. Behabtu, C. L. Pint, T. Liu, A. W. Orbaek, F. Mirri, J. Nam, A. R. Barron, R. H. Hauge, H. K. Schmidt, M. Pasquali, *J. Phys. Chem. B* **2012**, *116*, 6536–6542.
- [19] N. C. Schirmer, S. Ströhle, M. K. Tiwari, D. Poulikakos, *Adv. Funct. Mater.* **2011**, *21*, 388–21395.
- [20] R. Bhardwaj, X. H. Fang, P. Somasundaran, D. Attinger, *Langmuir* **2010**, *26*, 7833–7842.
- [21] Q. Yan, L. Gao, V. Sharma, Y.-M. Chiang, C. C. Wong, *Langmuir* **2008**, *24*, 11518–11522.
- [22] V. R. Dugyala, M. G. Basavaraj, *Langmuir* **2014**, *30*, 8680–8686.
- [23] V. L. Morales, J.-Y. Parlange, M. Wu, F. J. Pérez-Reche, W. Zhang, W. Sang, T. S. Steenhuis, *Langmuir* **2013**, *29*, 1831–1840.
- [24] M. Anyfantakis, Z. Geng, M. Morel, S. Rudiuk, D. Baigl, *Langmuir* **2015**, *31*, 4113–4120.
- [25] B. M. Weon, J. H. Je, *Phys. Rev. E* **2010**, *82*, 015305.
- [26] X. M. Lin, H. M. Jaeger, C. M. Sorensen, K. J. Klabunde, *J. Phys. Chem. B* **2001**, *105*, 3353–3357.
- [27] S. Narayanan, J. Wang, X. M. Lin, *Phys. Rev. Lett.* **2004**, *93*, 135503.
- [28] T. P. Bigioni, X.-M. Lin, T. T. Nguyen, E. I. Corwin, T. A. Witten, H. M. Jaeger, *Nat. Mater.* **2006**, *5*, 265–270.
- [29] P. J. Yunker, T. Still, M. A. Lohr, A. G. Yodh, *Nature* **2011**, *476*, 308–311.
- [30] M. Anyfantakis, D. Baigl, *Angew. Chem. Int. Ed.* **2014**, *53*, 14077–14081; *Angew. Chem.* **2014**, *126*, 14301–14305.
- [31] A. Crivoi, F. Duan, *Phys. Rev. E* **2013**, *87*, 042303.
- [32] D. M. Kuncicky, O. D. Velev, *Langmuir* **2008**, *24*, 1371–1380.
- [33] Y. Li, Z. Zhao, M. L. Lam, W. Liu, P. P. Yeung, C.-C. Chieng, T.-H. Chen, *Sens. Actuators B* **2015**, *206*, 56–64.
- [34] J. R. Trantum, M. L. Baglia, Z. E. Eagleton, R. L. Mernaugh, F. R. Haselton, *Lab chip* **2014**, *14*, 315–324.

Manuscript received: May 24, 2015
Final Article published: July 31, 2015